

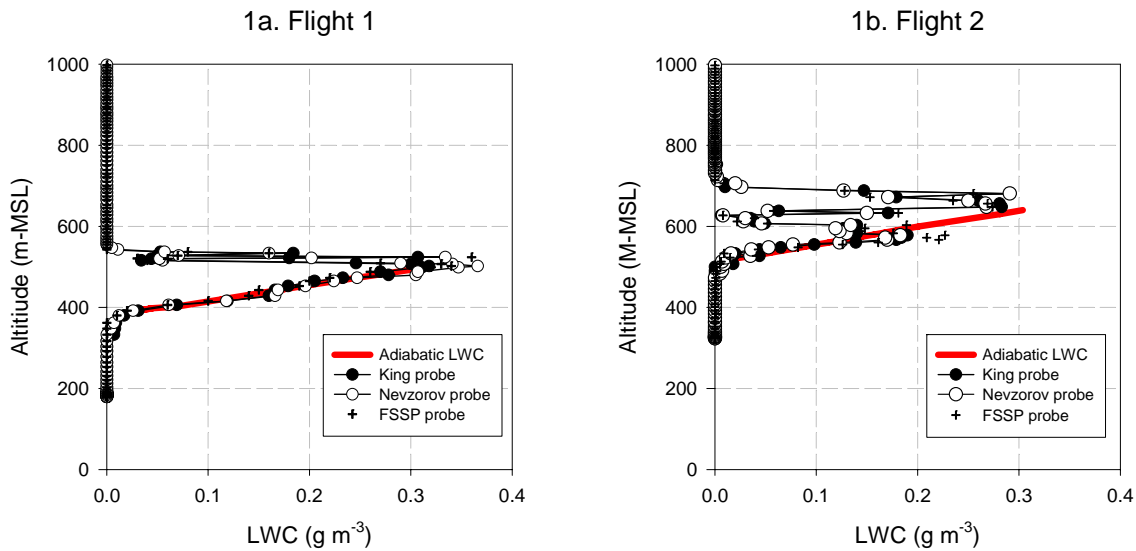
1 Supplement for
2
3 Cloud albedo increase from carbonaceous aerosol
4
5 W.R. Leaitch¹, U. Lohmann², L.M. Russell³, T. Garrett⁴, N.C. Shantz¹, D. Toom-
6 Sauntry¹, J.W. Strapp¹, K.L. Hayden¹, J. Marshall⁵, D. Worsnop⁶, J. Jayne⁶
7 1- Environment Canada, Toronto, Ontario, Canada M3H5T4
8 2 - ETH, Zurich, Switzerland
9 3 - Scripps Institute of Oceanography, University of California, San Diego, 92093,
10 U.S.A.
11 4 - University of Utah, Salt Lake City, Utah 84112-0110
12 5 - Max Planck Institute for Biogeochemistry, Jena, Germany
13 6 - Aerodyne Research, Inc., Billerica, MA 01821-3976
14
15 January 18, 2010

16 **Table S-1.** Component list for ion chromatographic analysis of the PILS sample

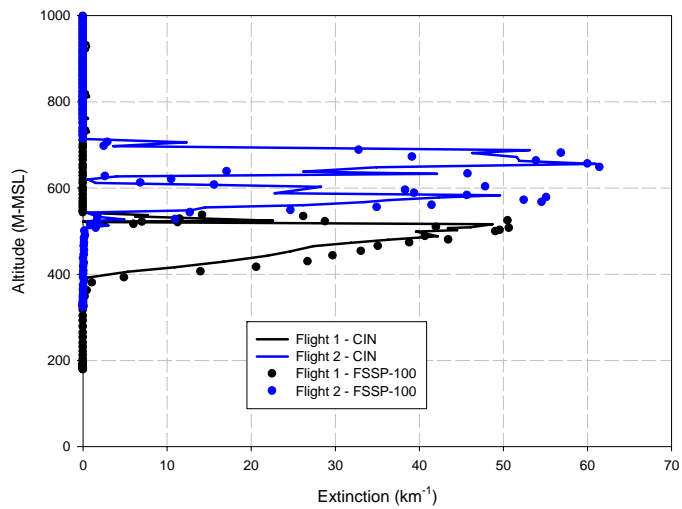
Component	Description
Dionex Ion Chromatographs	ICS 2000 with Eluent Generation, Temperature control and Degassing
Anions	
Eluent	25 mM Potassium Hydroxide - 10 min. inorganic analysis
Flow	1 ml/min
10-Port Valve	Alltech
Trace concentrator columns	TAC-ULP1 Ultra Low Pressure Trace Concentrator Column
Analytical and guard columns	AS11 HC & AG11 HC
Self Regenerating Suppressor	ASRS Ultra
Cations	
Eluent	25 mM Methanesulfonic Acid - 10 min. inorganic analysis
Flow	1 ml/min
10-Port Valve	Alltech
Trace concentrator columns	TCC-ULP1 Ultra Low Pressure Trace Concentrator Column
Analytical and guard columns	CS12 & CG12
Self Regenerating Suppressor	CSRS Ultra

17
18
19

20 **Figure S-1.** Comparison of the measurements of the cloud liquid water content (LWC)
21 with the adiabatic LWC for the profiles of flights 1 and 2. The measurements are from
22 the PMS King probe, the Nevezorov probe and the PMS FSSP-100 integrated droplet size
23 distribution. The adiabatic profiles are from the model calculations. The data from the
24 King probe are used for the calculations in the paper.

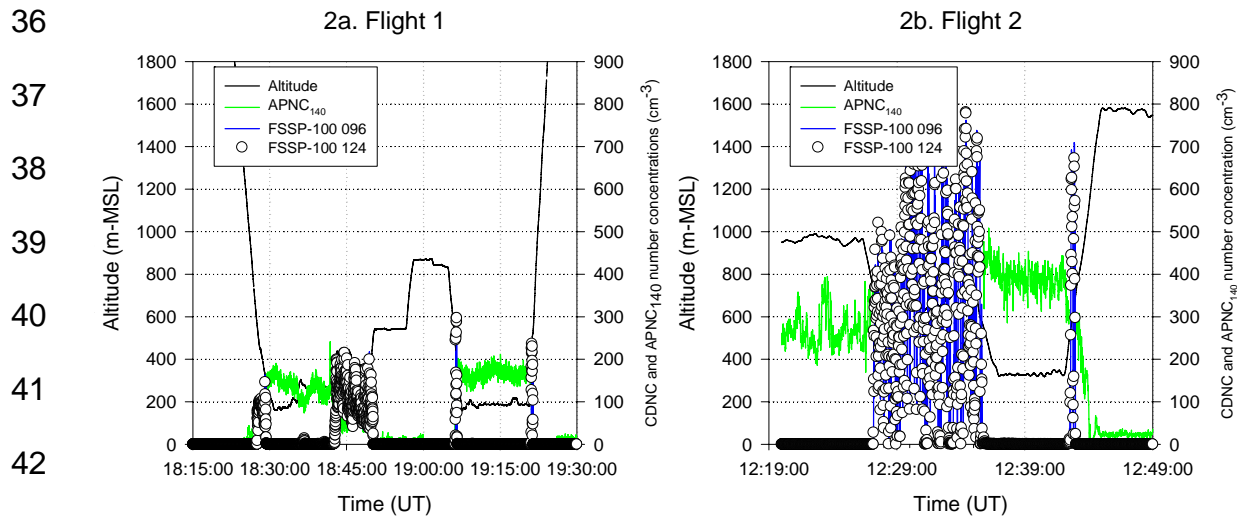


26 **Figure S-2.** Cloud light extinction measurements from the Gerber Cloud Integrating
27 Nephelometer (CIN) compared with the scattering coefficient calculated from the PMS
28 FSSP-100 droplet size distributions for the profiles of flights 1 and 2.

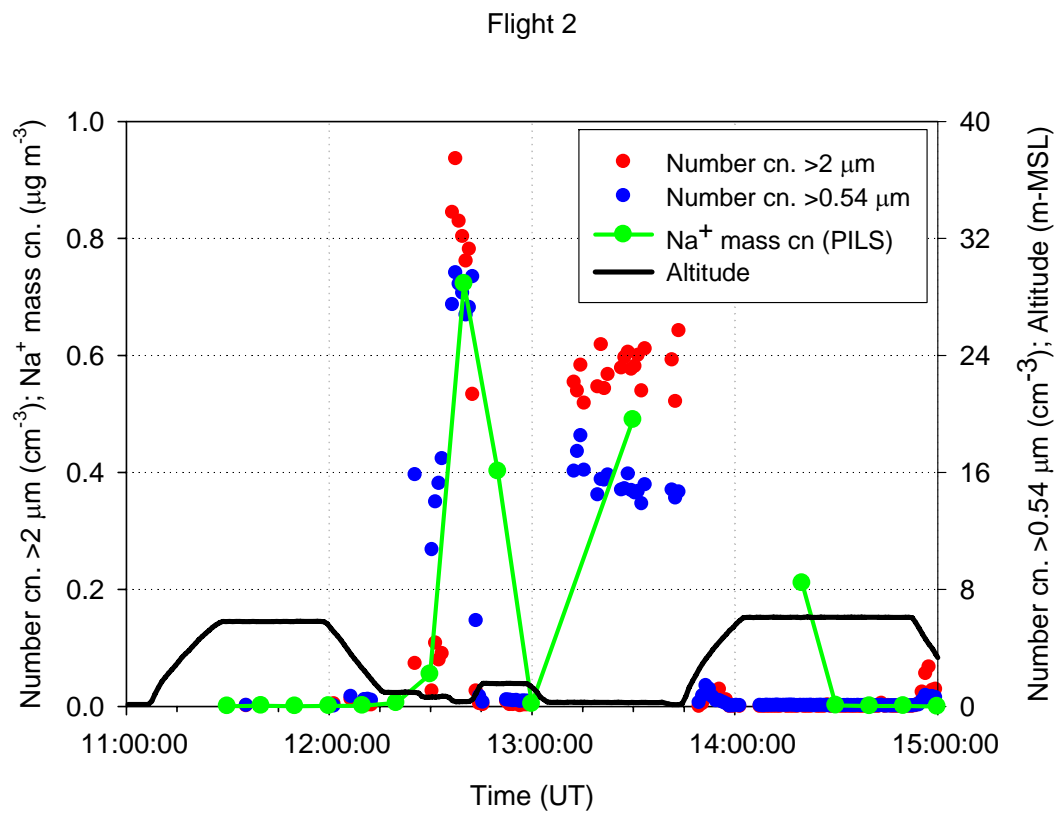


29

30 **Figure S-3.** Time series of altitude, aerosol particle number concentrations >140 nm
 31 (APNC_{140}) and cloud droplet number concentrations (CDNC) for flights 1 and 2.
 32 Observations are for the periods when cloud was profiled and sampling was conducted
 33 above, in and below cloud at level intervals. The CDNC are from the two FSSP-100
 34 probes (serial numbers 096 and 124) corrected for coincidence and probe dead times
 35 (Baumgardner et al., 1985), and the $\text{APNC}_{>140}$ is from the PCASP-100X.

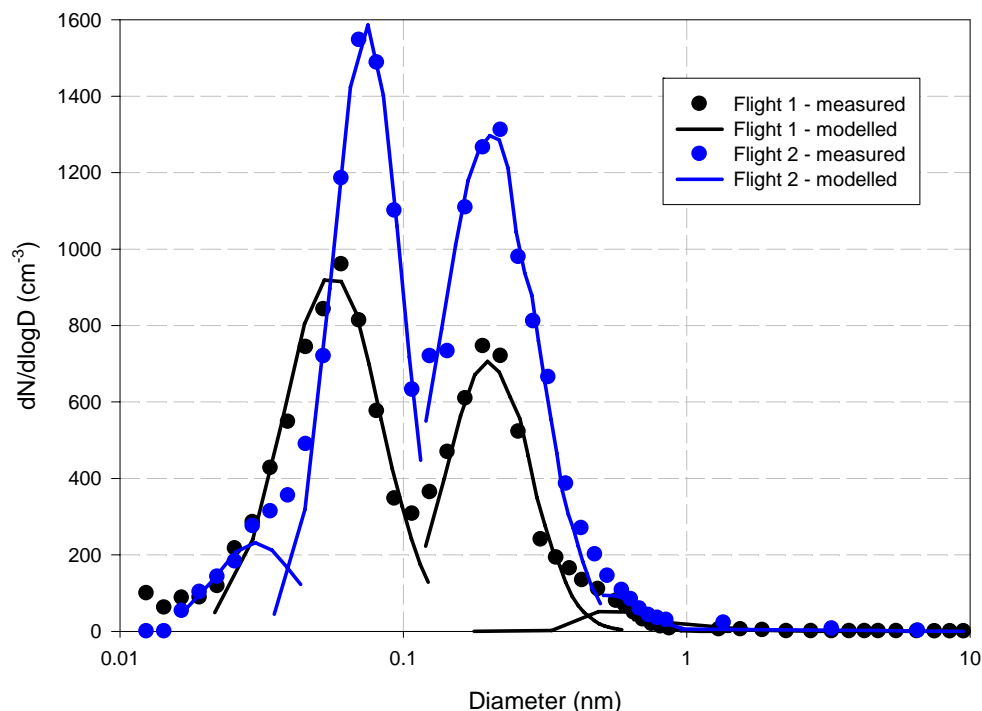


44 **Figure S-4.** Time series of sodium in the aerosol (measured with the PILS) and the
 45 number concentrations of particles $>0.54 \mu\text{m}$ aerodynamic diameter and $>2 \mu\text{m}$
 46 aerodynamic diameter for flight 2. The relative increase in particles $>2 \mu\text{m}$ at lower
 47 altitudes and the association of sodium with increased concentrations of these larger
 48 particles suggest the presence of sea salt particles.



49
 50

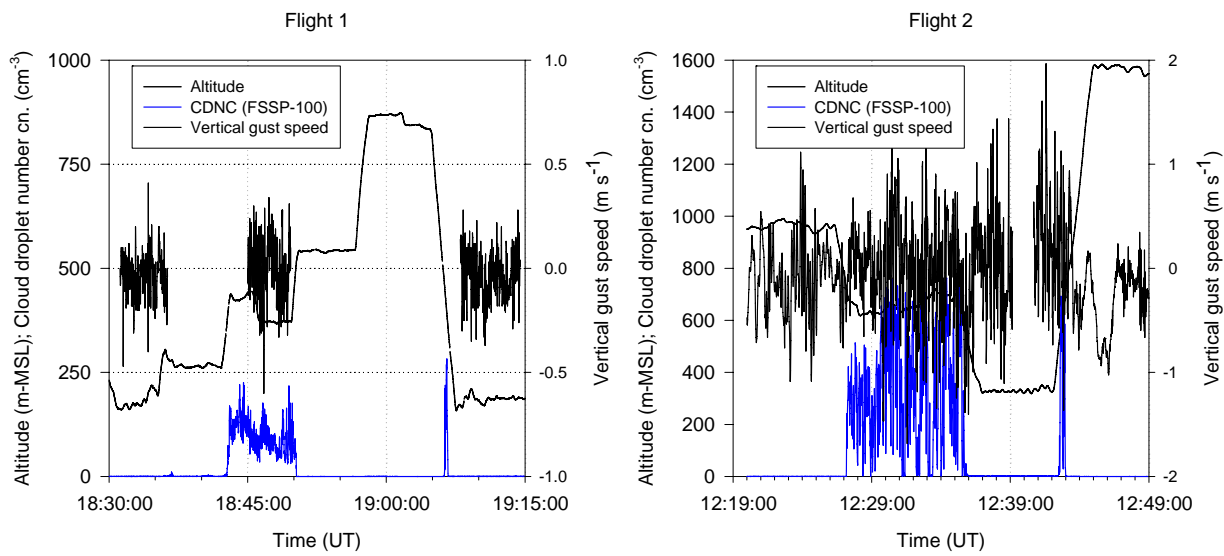
51 **Figure S-5.** Log-normal representation of measured cloud base aerosol size distributions
52 used for modelling.



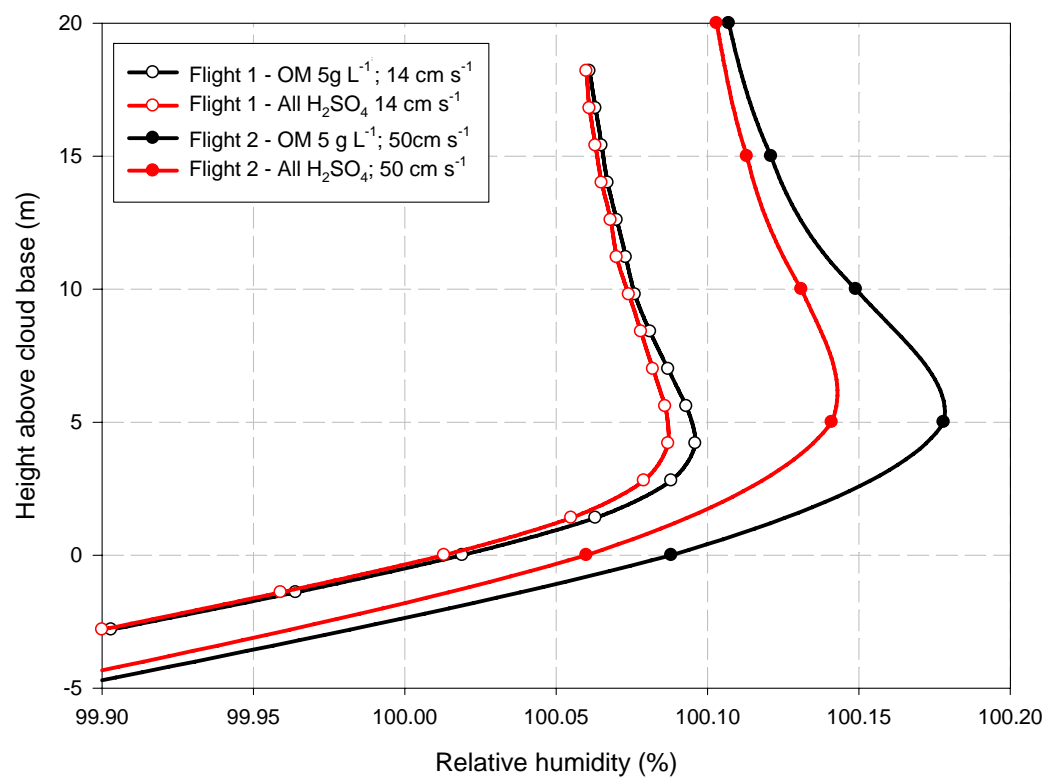
53

54 **Figure S-6.** Vertical gust speeds while flying level during flights 1 and 2. The values of
 55 one standard deviation of the measured gust speeds are 14 cm s^{-1} for flight 1 and 50 cm s^{-1}
 56 for flight 2; the means of the gust speeds for each flight segment are zero. The ranges
 57 of the gusts are approximately 20 cm s^{-1} for flight 1 and 100 cm s^{-1} for flight 2.
 58

59



60 **Figure S-7.** Examples of the simulated profiles of relative humidity just below and
61 above cloud base. The air is supersaturated with respect to water where the relative
62 humidity exceeds 100%. Cases of weak solubility of the OM (5 g L^{-1}) and pure H_2SO_4 are
63 shown for both flights 1 and 2. The water supersaturation decreases when the aerosol is
64 all sulphuric acid due to the more rapid rate of water uptake by this chemical component.



65
66
67